

# Bio-Inspired Fabrication of Porous Aromatic Framework-Coated Fabric for Achieving Durable Superhydrophobic Applications

Zhuojun Yan, Yimin Qiao, Na Li, Guiyue Zheng, Bo Cui, Xianghui Ruan, Yajie Yang, Naishun Bu,\* Ye Yuan,\* and Lixin Xia\*

Porous aromatic frameworks (PAFs) composed of high-density phenyl units are renowned for stable micro/meso-porous architecture and highly hydrophobic surface, which make them ideal candidates for durable superhydrophobic applications, especially under harsh conditions. Herein, a carbazole-based PAF solid is synthesized using carbazole and triphenylamine as the building units through the C–C linking pattern. For the first time, the PAF powder is uniformly deposited on the fabric surface via a facile dip-coating method, which thus shows superhydrophobicity with high water contact angle of 153.8° and oil contact angle of approximately 0°. Consequently, the PAF-coated fabric displays an outstanding simple oil/water mixture and separation efficiency of over 96% and enables simple and time-saving cyclic utilization at least 10 times. Due to the ultrahigh stability of PAF skeleton, the PAF-based composite maintains high superhydrophobicity under extreme conditions including high temperature, high humidity, and strong acidic/alkaline solutions. These results delineate important research advances toward the implementation of PAF powder in superhydrophobic applications.

## 1. Introduction

Superhydrophobic interfaces, defined by high water contact angle (WCA) value (>150°), have aroused wide interests for their practical utilization, such as water treatment, antifouling, and energy conversion.<sup>[1–5]</sup> With the increase in industrial demand, for instance, wastewater and oil spill accidents, the development of superhydrophobic substrates with high stability and durability is urgently demanded for effective separation and selective adsorption of oil pollution from water.<sup>[6–8]</sup> To cater to demand, various fabrication strategies have been investigated including electrospinning technique,<sup>[9]</sup> chemical etching,<sup>[10]</sup> self-assembly process,<sup>[11,12]</sup> hydrothermal method,<sup>[13]</sup> and others. However, great challenges of one-step production technique, moderate processing condition, and large-scale fabrication on diverse substrates still exist.<sup>[14]</sup> All of these problems refer to the absence of proper hydrophobic materials,

which lack durability, especially under extreme conditions of high temperature, strong acidity/basicity, and strong corrosion.<sup>[15,16]</sup>

Inspired by natural lotus and rice leaves, the rough surface gives an outward force to the attacked water droplet, forming a superhydrophobic interface. In the mechanism, an integrity of micro/nano-structured substrate renders low surface energy and creates a hydrophobic surface.<sup>[17]</sup> Porous aromatic frameworks (PAFs) are an important class of porous solids with rigid frameworks and ultra-high surface areas. Featuring the irreversible linking pattern (C–C bond), PAF solids keep their porous structure under harsh chemical conditions including acid/base, oxide, and moist environments. Through the above-planned analysis, PAF exhibits huge potential for hydrophobic applications because of the intrinsic merits including stable architecture, large surface area, and tunable porosity; particularly, the high-density phenyl units endow the highly superhydrophobic surface.<sup>[18–27]</sup>


In this contribution, a carbazole-based PAF network was synthesized using 2,7-dibromocarbazole and tris(4-boronic acid pinacol ester phenyl)amine as the building monomers through a Suzuki coupling reaction (**Figure 1**). Via a single-step fabrication process, the PAF powder was dispersed on the polyester fabric to obtain the superhydrophobic surface by dip-coating

Z. Yan, Y. Qiao, N. Li, G. Zheng, B. Cui, L. Xia  
College of Chemistry  
Liaoning University  
Shenyang 110036, P. R. China  
E-mail: lixinxia@lnu.edu.cn

X. Ruan, Y. Yang, Y. Yuan  
Key Laboratory of Polyoxometalate and Reticular Material Chemistry  
of Ministry of Education  
Northeast Normal University  
Changchun 130024, P. R. China  
E-mail: Yuany101@nenu.edu.cn

N. Bu  
School of Environmental Science  
Liaoning University  
Shenyang 110036, P. R. China  
E-mail: bunaishun@lnu.edu.cn

L. Xia  
Yingkou Institute of Technology  
Yingkou 115014, P. R. China

 The ORCID identification number(s) for the author(s) of this article can be found under <https://doi.org/10.1002/admi.202101994>.

DOI: 10.1002/admi.202101994



**Figure 1.** a) Synthesis route of PAF solid, LNU-41. b) Fabrication of PAF-coated fabric for oil/water separation.

deposition. Consequently, the PAF-based composite repelled water completely while allowing the permeation and adsorption of oil leading to the successful separation of oil from the oil/water mixture. In addition to the excellent recyclability, the as-prepared fabric withstood various harsh conditions such as high temperature, high humidity, and strong acidic/alkaline solutions. This work illustrates a versatile and simple approach using PAF powder to explore the durable superhydrophobic devices for the application under extreme conditions.

## 2. Results and Discussion

The formation of the PAF network LNU-41 was confirmed by Fourier transform infrared (FT-IR) and  $^{13}\text{C}$  solid-state NMR spectroscopy. The disappeared characteristic signals as  $500\text{ cm}^{-1}$  (C–Br stretching band) and  $1359\text{ cm}^{-1}$  (B–O stretching band) demonstrated the completeness of Suzuki coupling reaction (Figure S1, Supporting Information). As illustrated in  $^{13}\text{C}$  solid-state NMR spectrum (Figure S2, Supporting Information), the signal peaks observed at 110 and 139 ppm were attributed to the ortho aromatic methine carbon connected to the carbazole nitrogen (C–C) and the aromatic carbon bonded to the carbazole nitrogen (C–N), respectively. To further confirm the successful synthesis of LNU-41, series of structural groups are observed in Raman spectrum (Figure S3a, Supporting Information) including: C–N stretching vibration ( $1177\text{ cm}^{-1}$ ), benzene ring stretching vibration ( $1607\text{ cm}^{-1}$ ), N–H stretching vibration ( $1117\text{ cm}^{-1}$ ), and C–C bond stretching vibration of benzene ring ( $1324\text{ cm}^{-1}$ ). XPS survey spectroscopy confirms the presence

of C and N elements in the PAF network (Figure S3b, Supporting Information). In the deconvoluted C1s XPS spectrum (Figure S3c, Supporting Information), there are two characteristic peaks in LNU-41 sample centered at 284.9 and 283.8 eV attributed to the N linked carbon atom (in triphenylamine (TPA) and carbazole groups) and aromatic carbon atom (in benzene). As for N1s peak, it is deconvoluted into two significant peaks with binding energies of 399.8 and 399.3 eV corresponding to N atoms in respective TPA and carbazole units (Figure S3d, Supporting Information).<sup>[28,29]</sup> All these results proved the successful occurrence of Suzuki reaction and the structural integrity of PAF network.

The synthesized LNU-41 possessed an amorphous structure as revealed by the associated PXRD pattern (Figure S4, Supporting Information). Scanning electron microscopy (SEM) image showed that the PAF polymer exhibited a rough surface morphology of irregular particles with a uniform size distribution  $\approx 400\text{ nm}$  (Figure 2a). Transmission electron microscopy (TEM) presented a disordered worm-like structure and confirmed the amorphous nature of LNU-41 (Figure 2b). The thermal stability of LNU-41 PAF was investigated by thermogravimetric analysis (TGA) under air atmosphere. The TGA curve of LNU-41 did not show any significant weight loss till  $300\text{ }^\circ\text{C}$  (Figure S5, Supporting Information). LNU-41 PAF could not be dissolved or decomposed in various solvents including methanol, ethanol, acetone, dichloromethane, chloroform, DMF, and tetrahydrofuran, etc., which suggested ultrahigh chemical and thermal stability. The porosity of LNU-41 PAF was evaluated using  $\text{N}_2$  sorption isotherm measured at 77 K, which revealed a typical IV type reversible sorption profiles (Figure 2c).



**Figure 2.** a) SEM and b) TEM images for LNU-41 powder. c)  $N_2$  adsorption-desorption isotherm and d) pore size distribution curve by NL-DFT method for LNU-41 PAF.

The calculated Brunauer–Emmett–Teller (BET) surface area of LNU-41 was  $\approx 49 \text{ m}^2 \text{ g}^{-1}$ . Based on the non-local density functional theory (NL-DFT) model, LNU-41 PAF possessed both micro- (1.420 nm) and meso-pores (3.794 nm) (Figure 2d).

As depicted in SEM image, a smooth and flat morphology of flexible fabric is observed in Figure 3a; after coated with LNU-41 particles, the composite surface LNU-41 powder can be clearly observed on the surface and inside the fabric skeleton (Figure 3b). The irregularity of micro/nano-sized PAF particles brings about the voids on the surface of the flexible fabric. In addition, the microstructure of PAF network provides sufficient space for air trapping, which results in the superhydrophobicity of the LNU-41 coated fabric.<sup>[21–27]</sup> Meanwhile, these results also demonstrated that LNU-41 was successfully coated on the fabric. The hydrophobic property of LNU-41 coated fabric was tested by dropping water and chloroform droplets on the surface (Figure 3c). The WCA of uncoated fabric and the LNU-41 coated fabric were determined to be  $130.6^\circ$  (Figure S6a, Supporting Information) and  $153.8^\circ$  (Figure 3c inset). It can be seen that the ultra-high hydrophobic angle of  $156.8^\circ$  (Figure S6b, Supporting Information) of LNU-41 powder is well preserved after the coating of the fabric. This remarkable superhydrophobic surface is attributed to the cooperation effect of the micro/meso-porous structure, hydrophobic aromatic composition, and high particle roughness.

In the whole process of oil extraction, production, and utilization, oil pollution originated from oil spills and oily wastewater discharge seriously poisons environment to harm human health.<sup>[1–5]</sup> An effective oil/water separation method is urgently needed to reduce and control the discharge of oil. The PAF-coated superhydrophobic fabric repels the water phase and remains dry, which has a visible phenomenon of mirror after being immersed in water solution (Figure S7, Supporting Information). This phenomenon, known as the Cassie–Baxter wetting state, is attributed to the air layer trapped in the grooves of the superhydrophobic fabric. The above results show that the fabrics coated with LNU-41 are superhydrophobicity. Due to the pore structure with coexistence of micro/mesopores and superhydrophobic surface of PAF solid, LNU-41 easily removes oil and non-polar organic solvents from water without adsorbing water molecules.

Nine organic solvents were used to evaluate the adsorption capacity of superhydrophobic flexible fabric, as listed in Figure 3d. In the tests, the PAF-coated superhydrophobic fabric was immersed in the oils till a saturated adsorption, and then weighted to give the weight-based adsorption capacity. The adsorption capacity ( $k$ ) of superhydrophobic flexible fabric was calculated to be 3–8 times of different organic molecules of its weight. However, the uncoated fabric does not have a strong



**Figure 3.** SEM images for fabric a) before and b) after LNU-41 PAF coated. c) Water (dye with methylene blue) and chloroform (dye with methyl red) droplets on the LNU-41 PAF coated fabric, inset: water contact angle of the LNU-41 coated fabric. d) Adsorption capacities of superhydrophobic fabric coated with LNU-41 PAF for different oils and organic solvents.

adsorption capacity for oil, the adsorption capacity of uncoated fabric for dimethicone oil is  $\approx 5.73$  times its own weight. These large adsorption uptakes are ascribed to that the PAF is mainly composed of micropores (1–2 nm) and mesopores ( $>2$  nm), which are larger than the molecular length of all of the selected organic solvents. The oil droplets wet the superhydrophobic surface and are adsorbed by capillary action. The micro/mesoporous structure, high surface roughness, and a large number of aromatic rings in LNU-41 PAF enables the capillary effect for the adsorption of organic molecules.<sup>[30]</sup>

Taking into account the complicated environments, the stability of superhydrophobic surface is very critical for practical application. Therefore, the corrosion resistance of the superhydrophobic flexible fabric coated with LNU-41 PAF was tested by soaking the PAF-coated fabric in aqueous solutions with different pH and salinity for 24 h on the surface (Figure S8, Supporting Information). It was found that two droplets (pH = 1 and 13) remained spherical shape on the modified surface, which proved that the composite fabric owned good corrosion resistance. The high stability of LNU-41 coated fabrics may be due to the high rigidity of LNU-41's  $\pi$ - $\pi$  stacking framework and the weak contact of the superhydrophobic framework with

corrosive aqueous solutions.<sup>[31]</sup> The relationship between contact angle and superhydrophobic fabric coated with LNU-41 PAF was tested using water droplets with different pH values (Figure 4a). The contact angle decreased slightly with the change of pH value in the range of 144–156°. As for the temperature factors, the contact angles barely varied with the WCA values over 150° as the temperature increase from 25 to 145 °C (Figure 4b). The fabric is rolled up and folded in half more than 100 times to test the stability of LNU-41 powder attached fabric. The resulting fabric keeps the superhydrophobic quality as it is newly prepared (Figure S9, Supporting Information). These results proved that strong acidic/alkaline and high temperature showed little effect on the hydrophobicity of the PAF-coated fabric.

To evaluate the oil/water separation performance of the LNU-41 coated fabric, a mixture of 35 mL chloroform and 35 mL water is slowly poured into a gravity-driven oil/water separation device (Figure 5a,b). For clear observation, the oil and deionized water were dyed with methyl red and methylene blue, respectively. Because the density of chloroform is larger than water, the chloroform solvent in the underlying mixture penetrates the PAF-modified fabric quickly and flows into the



**Figure 4.** a) Water contact angles at different pH. b) Contact angles of the LNU-41 coated fabric at different temperatures (25, 45, 65, 85, 105, 125, and 145 °C).

container in a short time, while the water is isolated and saved above the fabric. In addition, the beaker for collecting the oil did not contain any blue color water, indicating that the surface of coated fabric still retained superhydrophobic property even after being wetted by oil.

To explore oil/water separation capacity of the LNU-41 coated fabric for different oil/water mixtures, several typical oils were used for this separation test. As shown in Figure 5e, the separation efficiency of the LNU-41 coated fabric for several organic solvents is more than 90%. This is attributed to the LNU-41



**Figure 5.** a,b) Photographs using LNU-41 coated fabric to separate the mixture of chloroform (dyed with methyl red) and water (dyed with methyl blue). Photographs of self-cleaning progress for the glass sheet c) before and d) after coated with LNU-41 powder. e) Separation efficiency of PAF-coated fabric for different organic solvents. f) Cycling performance for LNU-41 coated fabric.

powder doped on the fabric surface lowers the surface energy for organic phase. For a comparison, we used the uncoated fabric for oil/water separation and as seen in Figure S10, Supporting Information, and it has no capability to separate oil and water mixtures. In addition, recycling is also an important indicator for practical oil/water separation applications. After rinsing the superhydrophobic fabric with deionized water, the PAF-coated fabric was dried at 60–70 °C for recycling experiments. As shown in Figure 5f, the separation efficiency of the superhydrophobic flexible fabric is still over 93% after 10 times recycling experiments. Typically, oil flows through a hydrophobic filter fabric during oil/water separation, while water droplets are intercepted and collected on the fabric surface to generate water intrusion pressure. The LNU-41 coated fabric can withstand the water intrusion pressure of 0.97 KPa, indicating that its separation performance is relatively stable. This is mainly due to the presence of hydrophobic aromatic rings in the porous organic polymer backbone, which leads to the low surface energy of LNU-41. Also, the accumulation morphology of LNU-41 on the fabric surface and the pore nature can construct a highly rough surface, thus achieving superhydrophobicity of the coated fabric.<sup>[32,33]</sup> The excellent oil/water separation capability and recyclability of the composite fabric demonstrate the huge potential of PAF-based composite for achieving durable superhydrophobic applications.

In addition to separating simple oil/water mixtures, the superhydrophobic PAF-coated fabric reveals advanced capability in separating water-in-oil emulsions. The emulsions appear milky white, indicating that a large number of water droplets are distributed in the continuous oil phase. After separation by the superhydrophobic fabric, the solution became clear and transparent (Figure 6). This phenomenon proved that the oil and water phases in the water-in-oil emulsions were successfully separated. The separation efficiency was calculated to be 95.5%.

Further, we explored the self-cleaning properties of PAF solid by fixing the LNU-41 powder on the glass sheet. Compared with the uncoated glass sheets (Figure S11, Supporting Information) the water droplet on the LNU-41 coated with glass



**Figure 6.** Photograph of water-in-chloroform emulsions before and after the separation by using the superhydrophobic LNU-41 coated fabric.

sheet presents a nearly perfect spherical shape, manifesting the superhydrophobic surface of the modified glass. Since dust is a common outdoor pollutant, the self-cleaning performance of LNU-41 modified glass is carried out with dust as an object. During the sliding process of water droplets, the droplet is easily rolled away from the PAF-modified superhydrophobic coating. Moreover, the dust is immediately wrapped up and then washed away by the water droplets, leaving a clean surface (Figure 5d). This self-cleaning test indicates that the surface covered with LNU-41 has excellent superhydrophobic property. Both the low surface energy and the rough surface structure after coated with PAF powder on the surface render remarkable water-repellent property.<sup>[34]</sup>

### 3. Conclusions

In this contribution, a facile and versatile approach was determined to prepare superhydrophobic surface by dip-coating PAF powder on the substrates. The resulting composite fabric achieved high separation capability with efficiencies of 96% and 95.5% for oil/water mixture and water-in-oil emulsions, respectively. Notably, the obtained fabric withstood the extreme conditions such high temperature, high humidity, and strong acidic/alkaline solutions. This work opened up an avenue to fabricate PAF sample for superhydrophobic surface, which provided huge possibility for sewage treatments in the metallurgical, petrochemical, and pharmaceutical industries.

### 4. Experimental Section

**Materials:** 2,7-Dibromocarbazole (Aladdin), tris(4-boronic acid pinacol ester phenyl)amine (Sukailu), potassium carbonate, span-80 (Energy Chemistry), tetrakis(triphenylphosphine)palladium (TCI), *N,N'*-dimethylformamide (dry with calcium hydride before use, Sinopharm Chemical Reagent Co., Ltd), and all other materials were obtained from commercial suppliers and used without further purification.

**Characterization:** Fourier transform infrared spectroscopy (FT-IR) was performed using KBr pellets on a Shimadzu-Prestige 21 Fourier transform infrared spectrometer. Solid-state <sup>13</sup>C-NMR spectrum was measured on a Bruker AVANCE III 400 WB spectrometer at a MAS rate of 5 kHz. TGA was tested using a METTLER TOLEDO TGA/DSC 2 thermal analyzer under air atmosphere. Powder X-ray diffractometer (PXRD) measurement was carried out on a Bruker D8 QUEST diffractometer with Cu-K $\alpha$  radiation. X-Ray Photoelectron Spectroscopy (XPS) was performed on a K-Alpha XPS spectrometer (Thermo Fisher Scientific, MA, USA). SEM analysis was conducted on a SU8010 model scanning electron microscope with an accelerating voltage of 5 kV. TEM was recorded on a JEM-2100 with an accelerating voltage of 200 kV. N<sub>2</sub> adsorption isotherms were obtained on a Micromeritics ASAP 2460 instrument. Contact angle was measured by a contact angle meter (KRÜSS GmbH DSA1005, Germany). The water content in the collected filtrates and water-in-oil emulsions was determined by a Karl Fischer Titrator measurement (Mettler C30, Switzerland).

**Synthesis of LNU-41:** LNU-41 was synthesized via Suzuki coupling reaction (Figure 1a). Tris(4-boronic acid pinacol ester phenyl)amine (400 mg, 0.642 mmol) and 2,7-dibromocarbazole (313 mg, 0.963 mmol) were dissolved in 60 mL of *N,N'*-dimethylformamide (DMF) and then degassed by three freeze-pump-thaw cycles. Next, 5 mL of potassium carbonate (K<sub>2</sub>CO<sub>3</sub>, 2 M) and 80 mg (0.070  $\mu$ mol) of tetrakis(triphenylphosphine)palladium were quickly added into the



system. After degassing through three freeze-pump-thaw cycles, the mixture was stirred at 130 °C for 48 h. Cooling to room temperature, the residue was filtered and washed with tetrahydrofuran, distilled water, and acetone, respectively, to remove all the unreacted monomers and catalyst. Further purification of the product was carried out via Soxhlet extraction using tetrahydrofuran, dichloromethane, and chloroform in turns for 72 h. The product was dried in vacuum for 12 h at 90 °C to get LNU-41.

**Preparation of the Self-Cleaning Glass Sheet:** First, a clean glass piece was taken and a small piece of double-sided tape was stuck on the glass piece. After that, the LNU-41 powder was directly adhered to the surface of the glass piece by using double-sided tape.

**Preparation of the Superhydrophobic Fabric:** The superhydrophobic fabric was synthesized according to previous report with some modifications.<sup>[35,36]</sup> A piece of polyester fabric (40 × 40 mm) was ultrasonically cleaned in ethanol, deionized water, and acetone (40 mL) for 30 min to remove the stains and oils. After that, the fabric was dried in an oven at 60–70 °C and then immersed in 40 mL chloroform solution containing 30 mg LUN-41. The fabric was sonicated in chloroform solution for 4 h and dried to obtain a superhydrophobic flexible fabric coated with LNU-41.

**Oil Adsorption Capacity:** The weight gain (defined as the maximum mass of adsorbed oil divided by the mass of the PAF-coated fabric) is measured in order to evaluate the oil adsorption capacity of LNU-41. Weigh the flexible fabric coated with PAF, record it as  $w_0$ , then soak it in a mixture of water and oil (organic solvent). When the flexible fabric adsorption reaches saturation, it was taken out and weighed, recorded as  $w$ . The oil adsorption capacity ( $k$ ) of the PAF sample was calculated according to the Equation (1), which is expressed as:

$$k = \frac{w - w_0}{w_0} \quad (1)$$

**Preparation of Water-in-Oil Emulsions:** Water-in-oil emulsions are prepared according to the previous literature.<sup>[37]</sup> The span-80 was first dissolved in chloroform as the surfactant (2 mg mL<sup>-1</sup>), and then the water was added to the chloroform solution with the volume ratio of 1:99 (water and chloroform). Then, the mixture was subjected to vigorously stirring at 1000 rpm min<sup>-1</sup> for at least 4 h to obtain milky emulsion.

**Filtering Experiment:** Both simple oil/water mixtures and water-in-oil emulsions are separated in the same method. Take a simple oil/water mixture as an example: the fabric was first placed in the middle of the filtering apparatus and then oil/water mixture was poured from the top. The separation performance of oil dyed red and water dyed blue was recorded using a digital camera. The oil/water separation efficiency ( $r$ ) of the PAF coated fabric was determined and calculated according to the Equation (2), which is expressed as:

$$r(\%) = \frac{m_1}{m_0} \times 100\% \quad (2)$$

where  $m_0$  is the initial oil weight (g),  $m_1$  is the weight of oil collected from the oil/water mixture.

for water-in-oil emulsions, the separation efficiency ( $r$ ) should be calculated by Equation (3):

$$r(\%) = \left(1 - \frac{c_1}{c_0}\right) \times 100\% \quad (3)$$

where the  $c_1$  (mg L<sup>-1</sup>) represents the residual water content after the separation and  $c_0$  (mg L<sup>-1</sup>) represents the original water content in the emulsions.

**Intrusion Pressure Tests:** Before the test, the LNU-41 coated fabric was wetted with oil and installed into the filter, then, the water was slowly poured into the filter until the water started to pass through the fabric, and the corresponding water height was defined as the maximum water height. The intrusion pressure was calculated using the following Equation (4):

$$P_{\text{exp}} = \rho gh_{\text{max}} \quad (4)$$

where  $P_{\text{exp}}$  is the intrusion pressure,  $\rho$  is the density of water,  $g$  is the gravitational acceleration, and  $h_{\text{max}}$  is the maximum water height.<sup>[37]</sup>

## Supporting Information

Supporting Information is available from the Wiley Online Library or from the author.

## Acknowledgements

This work was supported by National Key Research and Development Project of China (2018YFC1801200), National Natural Science Foundation of China (31972522, 21704037, 21671089), Liaoning Revitalization Talents Program (XLYC2007032, XLYC2002097), Major Science and Technology Project of Liaoning Province (2019JH1/10300001), Scientific Research Fund of Liaoning Provincial Education Department (LQN202003, L2020002), Liaoning Provincial Natural Science Foundation (2021-MS-149, 2020-YKLH-22).

## Conflict of Interest

The authors declare no conflict of interest.

## Data Availability Statement

The data that support the findings of this study are available in the supplementary material of this article.

## Keywords

porous aromatic frameworks, superhydrophobicity, self-cleaning properties, oil/water separation

Received: October 13, 2021

Revised: April 7, 2022

Published online:

- [1] Z. L. Chu, Y. J. Feng, S. Seeger, *Angew. Chem., Int. Ed.* **2015**, *54*, 2328.
- [2] X. Du, S. J. You, X. H. Wang, Q. R. Wang, J. D. Lu, *Chem. Eng. J.* **2017**, *313*, 398.
- [3] J. F. Gao, X. W. Huang, H. J. Xue, L. C. Tang, R. K. Y. Li, *Chem. Eng. J.* **2017**, *326*, 443.
- [4] Q. Zhang, G. Gao, G. X. Lu, L. Shao, F. Shi, L. Jiang, M. J. Cheng, *Chem. Eng. J.* **2021**, *419*, 129766.
- [5] J. Li, L. Yan, H. Y. Li, W. J. Li, F. Zha, Z. Q. Lei, *J. Mater. Chem. A* **2015**, *3*, 14696.
- [6] F. Beshkar, H. Khojasteh, M. Salavati-Niasari, *J. Colloid Interface Sci.* **2017**, *497*, 57.
- [7] A. M. Rather, N. Jana, P. Hazarika, U. Manna, *J. Mater. Chem. A* **2017**, *5*, 23339.
- [8] F. Wu, K. Pickett, A. Panchal, M. X. Liu, Y. Lvov, *ACS Appl. Mater. Interfaces* **2019**, *11*, 25445.
- [9] D. Mitsunobu, G. Andreas, *Macromol. Mater. Eng.* **2018**, *303*, 1700621.
- [10] A. Kumar, B. Gogoi, *Tribol. Int.* **2018**, *122*, 114.
- [11] A. Checco, A. Rahman, C. T. Black, *Adv. Mater.* **2014**, *26*, 886.
- [12] S. Srinivasan, V. K. Praveen, R. Philip, A. Ajayaghosh, *Angew. Chem., Int. Ed.* **2008**, *47*, 5750.
- [13] X. J. Yue, J. X. Li, T. Zhang, F. X. Qiu, D. Y. Yang, M. W. Xue, *Chem. Eng. J.* **2017**, *328*, 117.

- [14] B. Wang, W. X. Liang, Z. G. Guo, W. M. Liu, *Chem. Soc. Rev.* **2015**, *44*, 336.
- [15] M. Li, Y. Li, F. Xue, X. L. Jing, *Appl. Surf. Sci.* **2019**, *480*, 738.
- [16] Q. H. Zeng, H. Zhou, J. X. Huang, Z. G. Guo, *Nanoscale* **2021**, *13*, 11734.
- [17] Y. H. Sun, Z. G. Guo, *Nanoscale Horiz.* **2019**, *4*, 52.
- [18] H. S. Sasmal, S. B. Chandra, P. Majumder, H. Kuiry, S. Karak, S. S. Gupta, R. Banerjee, *J. Am. Chem. Soc.* **2021**, *43*, 8426.
- [19] Y. B. Zhao, Y. Yuan, Y. M. Xu, G. Y. Zheng, Q. Zhang, Y. Q. Jiang, Z. Y. Wang, N. S. Bu, L. X. Xia, Z. J. Yan, *Nanoscale* **2021**, *13*, 1961.
- [20] Z. J. Yan, Y. Yuan, Y. Y. Tian, D. M. Zhang, G. S. Zhu, *Angew. Chem., Int. Ed.* **2015**, *54*, 12733.
- [21] D. Quéré, *Annu. Rev. Mater. Res.* **2008**, *38*, 71.
- [22] D. Bonn, J. Eggers, J. Indekeu, J. Meunier, E. Rolley, *Rev. Mod. Phys.* **2009**, *81*, 739.
- [23] X. J. Feng, L. Jiang, *Adv. Mater.* **2006**, *18*, 3063.
- [24] B. Bhushan, Y. C. Jung, *Prog. Mater. Sci.* **2011**, *56*, 1.
- [25] Y. B. Zhang, Y. Chen, L. Shi, J. Li, Z. G. Guo, *J. Mater. Chem.* **2012**, *22*, 799.
- [26] K. S. Liu, M. Y. Cao, A. Fujishima, L. Jiang, *Chem. Rev.* **2014**, *114*, 10044.
- [27] N. Gao, Y. Y. Yan, *Nanoscale* **2012**, *4*, 2202.
- [28] W. J. Li, F. Y. Yuan, N. Xu, S. W. Mei, Z. X. Chen, C. Zhang, *Electrochim. Acta* **2021**, *384*, 138344.
- [29] R. Kessel, J. W. Schultze, *Surf. Interface Anal.* **1990**, *16*, 401.
- [30] A. Li, H. X. Sun, D. Z. Tan, W. J. Fan, S. H. Wen, X. J. Qing, G. X. Li, S. Y. Li, W. Q. Deng, *Energy Environ. Sci.* **2011**, *4*, 2062.
- [31] L. Chen, C. L. Zhou, H. Yang, J. Lin, Y. Ge, W. Zhou, C. Y. Lu, L. X. Tan, L. C. Dong, *Chem. Commun.* **2021**, *57*, 11533.
- [32] N. Han, Z. Zhang, H. Gao, Y. Qian, L. Tan, C. Yang, H. Zhang, Z. Cui, W. Li, X. Zhang, *ACS Appl. Mater. Interfaces* **2020**, *3*, 6610.
- [33] Q. Sun, B. Aguila, J. A. Perman, T. Butts, F. S. Xiao, S. Q. Ma, *Chem* **2018**, *4*, 1726.
- [34] J. P. Zhang, L. Wu, B. C. Li, L. X. Li, S. Seeger, A. Q. Wang, *Langmuir* **2014**, *30*, 14292.
- [35] J. H. Lee, D. H. Kim, S. W. Han, B. R. Kim, E. J. Park, M. G. Jeong, J. H. Kim, Y. D. Kim, *Chem. Eng. J.* **2016**, *289*, 1.
- [36] S. Gupta, W. D. He, N. H. Tai, *Composites, Part B* **2016**, *10*, 99.
- [37] X. W. Huang, Z. F. Wu, S. Zhang, W. Xiao, L. L. Zhang, L. Wang, H. G. Xue, J. F. Gao, *J. Hazard. Mater.* **2022**, *429*, 12850.